Cement & Concrete Composites 33 (2011) 1014–1019

Contents lists available at ScienceDirect

Cement & Concrete Composites

journal homepage: www.elsevier.com/locate/cemconcomp

Determination of the bulk modulus of hydroxycancrinite, a possible zeolitic precursor in geopolymers, by high-pressure synchrotron X-ray diffraction

Jae Eun Oh [a,b], Simon M. Clark [c,d], Paulo J.M. Monteiro [a,*]

[a] Department of Civil and Environmental Engineering, University of California, Berkeley, CA 94720, USA
[b] School of Urban and Environmental Engineering, Ulsan National Institute of Science and Technology, Ulsan Metropolitan City, 689-798, South Korea
[c] Advanced Light Source, Lawrence Berkeley National Laboratory, Berkeley, California, CA 20015, USA
[d] Department of Earth and Planetary Sciences, University of California, Berkeley, CA 94720, USA

ARTICLE INFO

Article history:
Received 22 April 2010
Received in revised form 5 May 2011
Accepted 6 May 2011
Available online 14 May 2011

Keywords:
Hydroxycancrinite
High pressure
Geopolymer
Zeolite
X-ray diffraction
Equation of state
Bulk modulus

ABSTRACT

Crystalline zeolitic materials, such as hydroxycancrinite, hydroxysodalite, herschelite and nepheline, are often synthesized from geopolymerization using fly-ash and solutions of NaOH at high temperatures. Comprised mainly of 6-membered aluminosilicate rings that act as basic building units, their crystal structures may provide insight into the reaction products formed in NaOH-activated fly ash-based geopolymers. Recent research indicates that the hydroxycancrinite and hydroxysodalite may play an important role as possible analogues of zeolitic precursor in geopolymers. Herein is reported a high pressure synchrotron study of the behavior of hydroxycancrinite exposed to pressures up to 6.1 GPa in order to obtain its bulk modulus. A refined equation of state for hydroxycancrinite yielded a bulk modulus of $K_o = 46 \pm 5$ GPa (assuming $K'_o = 4.0$) for a broad range of applied pressure. When low pressure values are excluded from the fit and only the range of 2.5 and 6.1 GPa is considered, the bulk modulus of hydroxycancrinite was found to be $K_o = 46.9 \pm 0.9$ GPa ($K'_o = 4.0 \pm 0.4$, calculated). Comparison with the literature shows that all zeolitic materials possessing single 6-membered rings (i.e., hydroxycancrinite, sodalite and nepheline) have similar bulk moduli.

1. Introduction

Recent research on geopolymers has demonstrated that these materials may be used as an alternative binding material to Portland cement. Their potential as the new building block for 'green concrete' has resulted in increased interest in this topic [1]. The alkali-activation of glassy alumino-silicate materials produces materials, known as geopolymers, that have strong binding properties [2]. Current research on geopolymers has focused on using industrial waste materials (e.g., coal fly ash) as source materials as the recycling of these materials has substantial economic and environmental benefits (see Table 1).

Although many studies have concluded that geopolymers can be viewed as an analogue of zeolite [1,3], comparatively little is known about their atomistic structure because geopolymers are basically amorphous. Having said that, the geopolymeric reaction often forms zeolitic phases in their matrices (see Table 1). Given the difficulty due to the amorphous structure of geopolymers, valuable information on the structural identity of geopolymers can be obtained by comparing geopolymers with those zeolitic phases. Note that while geopolymers are basically amorphous, they also form crystalline phases.

Table 1 lists the most frequently observed crystalline phases common to geopolymers [e.g., hydroxysodalite, herschelite (=Na—chabazite), and hydroxycancrinite], which belong to the same zeolite framework type known as the 'ABC-6 family', when fly ash was activated by NaOH (or a mixture with Na—silicate) solution [15]. Based on this observation, the geopolymer reaction product, also called the zeolitic precursor, was hypothesized to possess a similar structure as the ABC-6 family of zeolite minerals when a high concentration of Na-based alkali-activating solution is used [14]. This proposition is also supported by the fact that ^{29}Si NMR spectrum of aged fly ash geopolymers is identical to herschelite [16].

Similarly, those zeolitic phases have been also observed in zeolite synthesis studies. The science of zeolite synthesis through the use of coal fly ash has been regarded as an analogue of fly ash-based geopolymer synthesis [17]: both possess similar methodologies of synthesis in terms of the type of alkali-activator, and the concentration of the activator and source materials. Even though zeolite synthesis requires a more dilute system and higher temperatures (between 150 and 200 °C), the reaction mechanisms in both cases are similar. Earlier zeolite synthesis studies used high concentrations (>5 M) of NaOH solution (or with a mixture of sodium

* Corresponding author.
E-mail address: monteiro@berkeley.edu (P.J.M. Monteiro).

0958-9465/$ - see front matter © 2011 Elsevier Ltd. All rights reserved.
doi:10.1016/j.cemconcomp.2011.05.002

Table 1
Crystalline zeolite phases of geopolymers as found in the literature.

Reference	Crystalline phases	Material and solution
Palomo et al. [1]	Hydroxysodalite	Fly ash F, NaOH, Na—silicate
Krivenko and Kovalchuk [4]	Hydroxysodalite, analcime	Fly ash F, NaOH, Na—silicate
Criado et al. [5]	Hydroxysodalite, Na—chabazite (=herschelite), sodium bicarbonate	Fly ash F, NaOH, Na—silicate
Bakharev [6]	Hydroxysodalite, chabazite, zeolite Na—P1	Fly ash F, NaOH, Na—silicate
Bakharev [7]	Hydroxysodalite, trace of chabazite, zeolite Na—P1, zeolite A	Fly ash F, NaOH, Na—silicate
Fernandez-Jimenez et al. [8]	Hydroxysodalite, herschelite-type mineral	Fly ash F, NaOH
Bakharev [9]	Hydroxysodalite, nepheline, zeolite Na—P1	Fly ash F, NaOH, KOH, Na—silicate
Criado et al. [10]	Sodalite, Na—chabazite, zeolite P(Na), zeolite Y (=faujasite variant)	Fly ash F, NaOH, Na—silicate
Dombrowski et al. [11]	Sodalite, nepheline	Fly ash F, NaOH, Ca(OH)2
Fernandez-Jimenez et al. [12]	Hydroxysodalite, Na—chabazite (=herschelite), analcime	Fly ash F, NaOH, Na—silicate
Alvarez-Ayuso et al. [13]	Sodalite, chabazite, faujasite, zeolite Na—P1, zeolite 4A (=zeolite A)	Fly ash F, NaOH
Oh et al. [14]	Hydroxycancrinite, hydrotalcite	Fly ash F, NaOH

silicate) for the alkaline activation of coal fly ash as a source material, frequently resulting in specific types of zeolitic materials, such as nepheline, herschelite (=Na-chabazite), hydroxysodalite, and hydroxycancrinite. These belong to the ABC-6 family of zeolite framework except for nepheline, which also consists of 6-membered rings without stacking manner of the ABC-6 family framework. Lower concentrations (0.5–3 M) of NaOH solution result primarily in zeolite Na—P1 and analcime [18–22]. Note that the lower concentration of NaOH solution within a range of up to 12 M usually results in the lower strength of geopolymer matrix [23], implying less formation of geopolymeric gel in the matrix. Given the similarity between geopolymerization and zeolite synthesis in terms of NaOH concentration, zeolite Na—P1 and analcime could be less related to geopolymeric gel than nepheline, herschelite, hydroxysodalite, and hydroxycancrinite.

The basic building unit forming the ABC-6 family zeolites is a 6-membered ring, consisting of Al- and Si-tetrahedra (see Fig. 1). Among the entire 176 zeolite framework types [15], only 19 members of zeolite framework types can be described as belonging to the ABC-6 family. What differentiates these specific zeolites is the stacking sequence of the 6-membered rings. If the position of one 6-membered ring on a certain layer is called 'A', and the two possible positions of the ring on the next above layer are called 'B' and 'C', respectively, all the stacking sequences of the basic layers constituting the ABC-6 group of minerals can be described by 'AB', 'ABC', or 'AABB', and so on. For example, hydroxycancrinite has the 'ABAB' arrangement, while chabazite follows the 'AABBCC' arrangement [24]. Previous geopolymer researchers have noted the large presence of hydroxysodalite as a crystalline phase in the case of high concentration of NaOH solution (>5 M) [5–7,9]. Recent research by Oh et al. [14] has shown strong evidence of a hydroxycancrinite phase also forming in the geopolymer matrix made from similar synthesizing conditions, suggestion the need for more study on hydroxycancrinite. Given that the stacking sequence of periodic building unit of hydroxycancrinite (=ABAB... sequence) is the closest to that of hydroxysodalite (=ABCABC... sequence), and that both minerals also have the simplest sequence combinations among the ABC-6 family zeolites resulting in similar X-ray diffraction (XRD) patterns [15], it is not surprising that earlier research might have mistaken some signals of hydroxycancrinite for that of hydroxysodalite.

First reported by Khomyakov et al. in 1992, hydroxycancrinite is a naturally occurring zeolite, with an isomorphic crystal structure similar to a synthetic 'basic cancrinite' [25]. Hydroxycancrinite $\{Na_8[AlSiO_4]_6(OH)_2{\cdot}2H_2O\}$ belongs to the cancrinite framework in ABC-6 family, possessing a hexagonal crystal system with lattice parameters $a = 12.740(3)$, $c = 5.182(2)$ Å, and space group of $P3$. The schematic view of crystal structure of hydroxycancrinite is shown in Fig. 2.

Given the marked similarities between geopolymerization and zeolite synthesis, the zeolitic precursor must share some structural similarities with the ABC-6 family of zeolite minerals. Therefore, hydroxysodalite and hydroxycancrinite—having the simplest

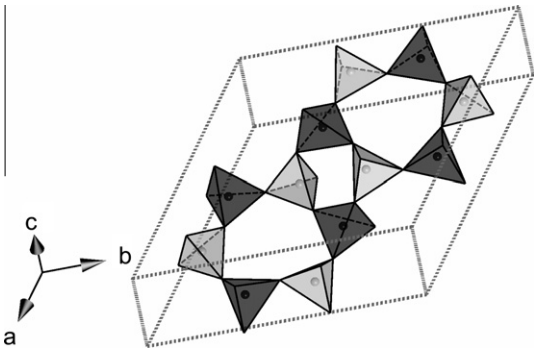

Fig. 1. Two (single layer) 6-membered rings; the dark gray indicates Al-tetrahedra, and light gray implies Si-tetrahedra. This figure is a part of a hydroxycancrinite.

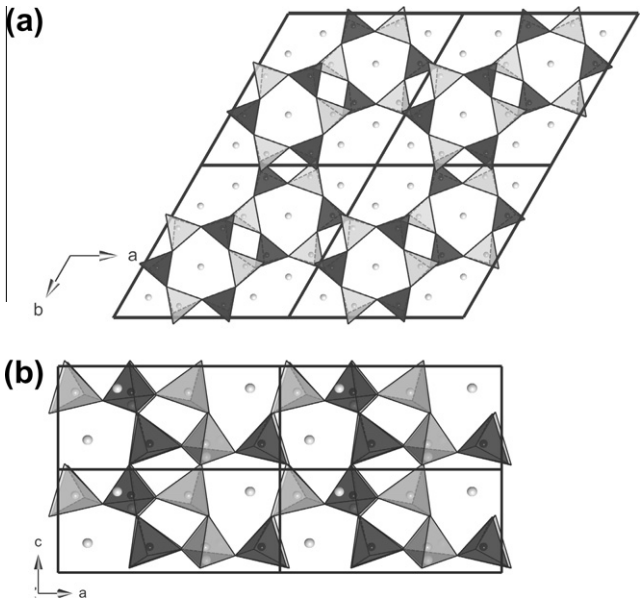

Fig. 2. Schematic crystal structure of hydroxycancrinite. (a) Projection of structure seen along [0 0 1] and (b) projection seen along [0 1 0] showing (AB) arrays of 6-membered rings. The dark gray indicates Al-tetrahedra, while light gray shows Si-tetrahedra, and sodium atoms are shown as spheres.

atomic arrangement (AB) among zeolites belonging to the ABC-6 family framework type—emerge as strong candidates to represent the crystal structure of a zeolitic precursor of a geopolymer; the level of similarity is as comparable as tobermorite and jennite are to C—S—H in the cement science.

Several studies investigated the elastic property (e.g., elastic modulus or bulk modulus) of geopolymers using nanoindentation [26,27] or macroscale compressive tests [28–32]; unfortunately, the obtained values had a large variance. Currently, only limited nanoindentation results for geopolymer are available. Němeček et al. [26] measured the elastic modulus of coal fly ash-based geopolymer as $E = 17.7$ GPa, and Škvára et al. [27] reported a value of $E = 36.1 \pm 5.1$ GPa, which was measured for a mixed phase of C—S—H from activated slag and fly ash-based geopolymer. Even while acknowledging that these two values cannot be directly compared because the sample materials conditions were different (i.e., geopolymer vs. geopolymer with C—S—H), the difference was still large. This difference may be interpreted as a consequence of nano-size of impurities intermixed with geopolymer gel, evidenced by the considerable amount of nano-pores below 1 nm size [26,33] or unreacted fly ash particles present in hardened geopolymer [26]. Bell et al. [33] reported that geopolymers made from natural metakaolin contained ~40% of porosity (volume%), with an average pore radius of ~3.4 nm. When they used a synthetic alumino-silicate metakaolin, the average pore size of geopolymers was reduced to ~0.8 nm with a ~40% porosity. Because the characteristic length of the nanoindentation area is in the order of $\sim 10^{-6}$–10^{-7} m, those nano-pores may be included in the indented area and could affect the measured elastic modulus values. Furthermore, the accuracy of the nanoindentation results highly depends on the size of homogeneous geopolymer phase in the geopolymer samples. If the size of homogenous geopolymer phase is much smaller than the area of nanoindentation, the result could be distorted by the neighboring unreacted fly ash particles [34]. Obviously, a novel experimental technique is necessary for accurate measurement of the intrinsic property of elasticity of geopolymers.

The current study employed high pressure X-ray diffraction with the aim of investigating the bulk modulus. Hydroxycancrinite was chosen to represent the zeolitic precursor of geopolymer among the ABC-6 family. The obtained bulk modulus may be used in mechanical simulation studies as an important material property for geopolymer studies. Another strong candidate of zeolitic precursor is hydroxysodalite, which will be examined in subsequent research. Not only was this the first experimental measurement of a bulk modulus of hydroxycancrinite itself, it was also the first of a geopolymer-related material.

2. Experimental

The high pressure powder X-ray diffraction experiment was carried out at beamline 12.2.2 of the Advanced Light Source [35], using a synchrotron monochromatic X-ray beam with $\lambda = 0.495929$ Å (=25 keV energy). The National Bureau of Standards LaB_6 powder diffraction standard was used to calibrate the working distance between sample and detector. Diffraction patterns were recorded by a MAR345 image plate (3450 × 3450 pixels), with an exposure time of 300 s at room temperature and analyzed using the FIT2D [36], XFIT [37] software programs.

First, the sample was finely ground, mixed with an enough amount of pressure-transmitting liquid medium (4:1 Methanol/Ethanol solution) filling up a small sample chamber, and then placed into the chamber in a steel gasket in the diamond anvil cell (DAC) (see Fig. 3). The 4:1 Methanol/Ethanol solution has been most widely used as a liquid medium to generate a hydrostatic pressure condition in high pressure experiments and it has a nominal hydrostatic pressure limit of 10 GPa [38]. The sample chamber size was 180-μm diameter with 75-μm thickness. The pressure inside the sample chamber was determined using the ruby (Al_2O_3 doped with Cr^{3+} (0.05%)) fluorescence calibration method [39]. The pressure was increased up to 6.1 GPa in a hydrostatic condition. After the sample underwent interpretation of XRD patterns, the crystal used for this study—from Lovozero Massif, Kola Peninsula, Russia—turned out to be a mixture of hydroxycancrinite and natrolite.

3. Results and discussion

The two-dimensional high pressure powder X-ray diffraction patterns measured in the present study were integrated to one-dimensional diffraction profiles (see Fig. 4). The hydroxycancrinite are labeled with solid stars (★).

Presented in Table 2 with corresponding plots in Fig. 5, the evolution of lattice parameters and volumes for the hydroxycancrinite under high pressure were calculated using the unit cell refinement software Celref [40].

The bulk modulus value was obtained by curve-fitting of the pressure-normalized volume data using a third-order Birch–Murnaghan equation of state (B–M EoS), which is expressed as:

$$P = \frac{3}{2}K_o\left[(V/V_o)^{-\frac{7}{3}} - (V/V_o)^{-\frac{5}{3}}\right]\left[1 + \frac{3}{4}(K_o' - 4)\left((V/V_o)^{-\frac{2}{3}} - 1\right)\right]$$

where V is volume of unit cell under increased pressure, V_o the initial volume of unit cell at ambient pressure, P the pressure applied

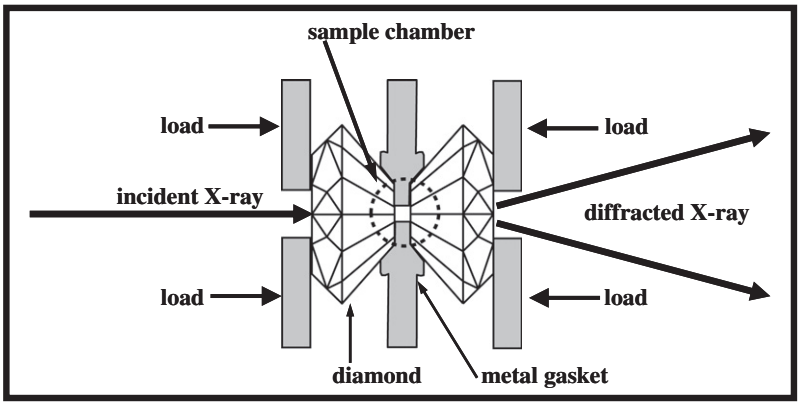

Fig. 3. Schematic view of high pressure X-ray diffraction using a diamond anvil cell.

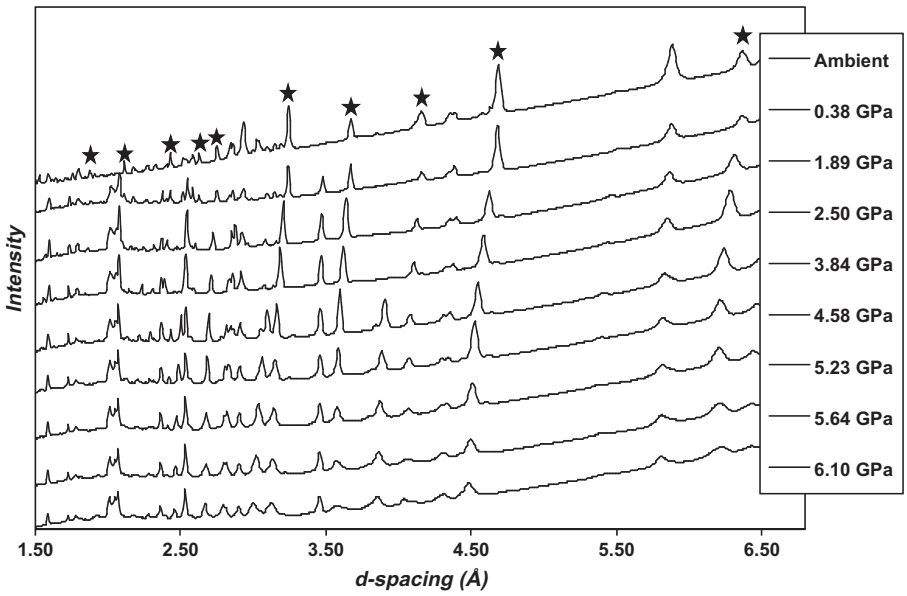

Fig. 4. Observed one-dimensional X-ray diffraction patterns of hydroxycancrinite (label ★) under increasing pressure.

Table 2
Unit cell lattice parameters for hydroxycancrinite under pressure.

P (GPa)	V (Å^3)	Lattice parameters	
		a (Å)	c (Å)
0.0 ± 0.0	727.48 ± 0.02	12.73 ± 0.02	5.18 ± 0.01
0.4 ± 0.2	725.81 ± 0.03	12.73 ± 0.02	5.18 ± 0.01
1.9 ± 0.2	703.38 ± 0.04	12.61 ± 0.02	5.10 ± 0.02
2.5 ± 0.3	691.42 ± 0.05	12.56 ± 0.02	5.06 ± 0.02
3.8 ± 0.3	675.67 ± 0.04	12.47 ± 0.02	5.02 ± 0.02
4.6 ± 0.4	667.58 ± 0.06	12.43 ± 0.03	4.99 ± 0.02
5.2 ± 0.4	661.76 ± 0.09	12.41 ± 0.05	4.97 ± 0.04
5.6 ± 0.4	657.99 ± 0.08	12.39 ± 0.07	4.95 ± 0.05
6.1 ± 0.5	652.6 ± 0.1	12.36 ± 0.09	4.93 ± 0.07

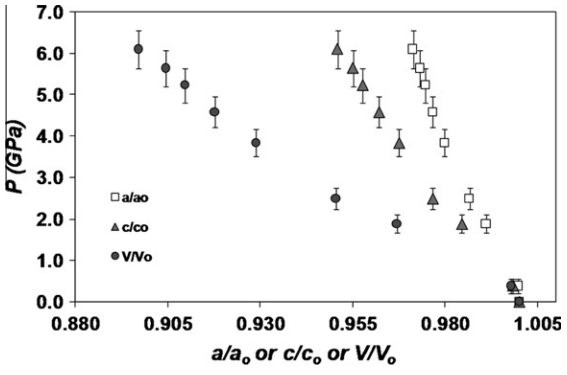

Fig. 5. Changes in the normalized lattice parameters and volume of hydroxycancrinite under pressure (a_o and c_o are the initial lattice parameters of a and c at ambient pressure).

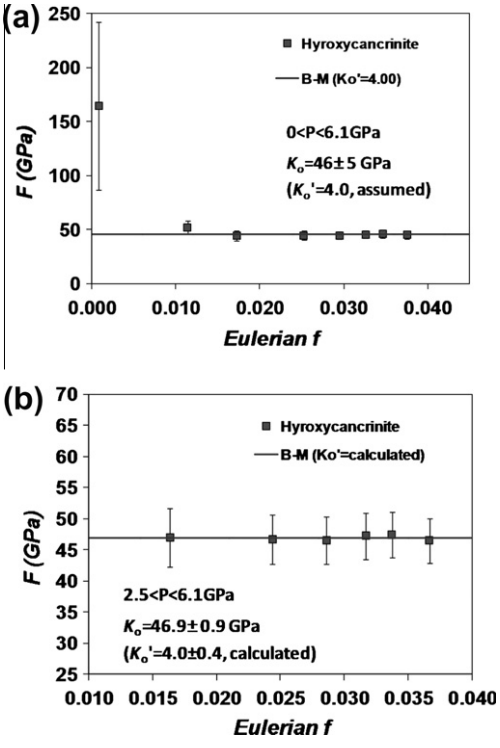

Fig. 6. Plot of Eulerian strain, $f = 0.5\cdot[(V/V_o)^{-2/3} - 1]$, vs. the normalized pressure, $F = P/\{1.5[(V/V_o)^{-7/3} - (V/V_o)^{-5/3}]\}$ for hydroxycancrinite: (a) f–F plot for the entire pressure range $0 < P < 6.1$ GPa; and (b) f–F plot for the pressure range $2 < P < 6.1$ GPa. For (b), the calculated unit cell volume V_o is obtained by g–G plot [43].

to material, K_o the bulk modulus at zero pressure, and K'_o the pressure derivative of bulk modulus at zero pressure [41–43].

By setting the normalized pressure, $F = P/\{1.5[(V/V_o)^{-7/3} - (V/V_o)^{-5/3}]\}$, and the Eulerian strain, $f = 0.5\cdot((V/V_o)^{-2/3} - 1)$, the third order Birch Murnaghan equation of state is reformed into the linear form: $F(f) = K_o - 1.5K_o(4 - K'_o)f]$.

In the plot of F vs. f, the y-intercept and the slope of the weighted least-squares fit gives the bulk modulus K_o and its pressure derivative K'_o at zero pressure [41]. As is usual, the K'_o was assumed to be 4. Low-range pressure studies [44] and zeolite studies [45] make this assumption because the pressure derivative K'_o values for many materials appear near 4. A weighted linear least-squares fits with errors [46] was applied to give less weights to the data with large error bars in calculation.

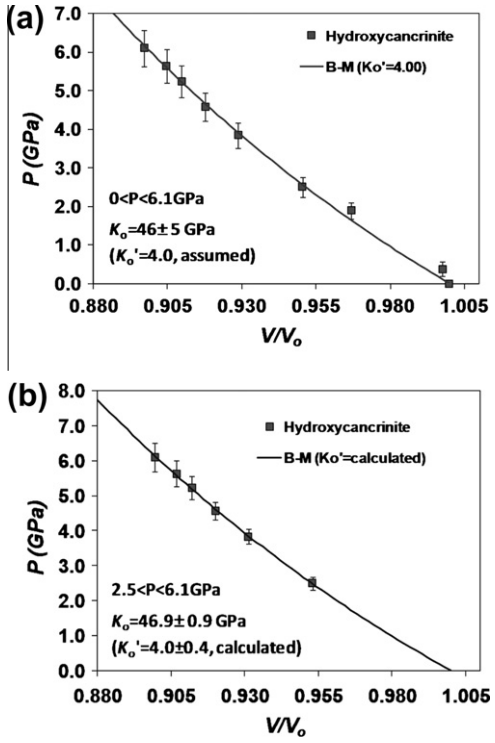

Fig. 7. Pressure-normalized volume data of hydroxycancrinite and its curve-fitting with third order Birch–Murnaghan equation of state: (a) curve-fitting including all pressure range by fixing $K'_o = 4.0$ and (b) curve-fitting excluding data points below 2 GPa, resulting in more accurate value.

The B–M EoS curve-fitting for the entire pressure range resulted in a bulk modulus for hydroxycancrinite as $K_o = 46 \pm 5$ GPa [note: K'_o was assumed to be 4.0 because the B–M EoS curve-fitting produced somewhat low value of 2, as shown in Figs. 6a and 7a]. The measured pressure–volume data showed a peculiar deviation from the refined B–M EoS curve between 0 and 1.9 GPa. Therefore, a further B–M EoS curve-fitting was applied to only the volume data over 2.5 GPa by employing a calculated unit cell volume of ambient pressure (V_o) obtained from g–G plot [43]. This allows for obtaining the bulk modulus by only using measured high pressure data without ambient pressure–volume data (i.e., V_o). The newly refined bulk modulus (with volume data measured between 2.5 and 6.1 GPa) is $K_o = 46.9 \pm 0.9$ GPa, with a calculated value of $K'_o = 4.0 \pm 0.4$ [see Figs. 6b and 7b].

Note that bulk moduli of other zeolitic materials that form in fly ash Class F based geopolymers (see Table 1) and unreacted raw material phases from the literature (see Table 3) can be used for mechanical simulation studies for geopolymers. Zeolitic materials consisting of only single 6-membered rings (see Fig. 1), which include hydroxycancrinite, sodalite and nepheline, have similar bulk modulus values within comparable range (46–52 GPa) [49]. All these materials have Si/Al = 1; whereas chabazite (with only double 6-membered rings) has Si/Al = 2; its bulk modulus is higher than others. Given that these zeolitic materials formed frequently in similar geopolymerization conditions (i.e., high NaOH concentration), this may explain why Duxon et al. [32] observed that Young's modulus of metakaolin-based geopolymer increased proportionally to Si/Al ratio, and the highest value appeared at —Si/Al = 2.

4. Conclusions

Hydroxycancrinite (Si/Al = 1) was studied as an analogue of potential geopolymer forming materials using high pressure synchrotron X-ray diffraction. The bulk modulus of hydroxycancrinite was calculated as $K_o = 46 \pm 5$ GPa (assuming $K'_o = 4.0$) for the entire measured pressure–volume data. Because the experimental pressure–volume data showed some deviation from the obtained B–M EoS curve below 2.5 GPa, a further bulk modulus was calculated using only the pressure range between 2.5 and 6.1 GPa and it was found to be $K_o = 46.9 \pm 0.9$ GPa with a fine calculated value of $K'_o = 4.0 \pm 0.4$. Both bulk modulus values agree generally with results for other zeolitic materials—sodalite and nepheline (Si/Al = 1)—consisting of only single 6-membered rings. These zeolitic materials made of single 6-membered rings show less bulk modulus values than that of chabazite (Si/Al = 2) with double 6-membered rings. This trend may explain why the higher Si/Al produced the higher Young's modulus of hardened geopolymer paste up to Si/Al = 2.

Acknowledgements

This publication was based on work supported in part by Award No. KUS-l1-004021, made by King Abdullah University of Science and Technology (KAUST). The Advanced Light Source is supported by the Director, Office of Science, Office of Basic Energy Sciences, of the U.S. Department of Energy under Contract No. DE-AC02-05CH11231.

Table 3
Bulk modulus values of crystalline phases found in fly ash-based geopolymer from the literature.

Group	Phase	Al/Si	K_o (GPa) or E(GPa)	K'_o	Reference
Zeolite with 6-membered rings (ABC-6 family)	Hydroxy-cancrinite	1.0	$K_o = 46 \pm 5$ (0 < P < 6.1 GPa) $K_o = 46.9 \pm 0.9$ (2.5 < P < 6.1 GPa)	4 (fixed) 4.0 ± 0.4	*
	Sodalite	1.0	$K_o = 52 \pm 8$	4 (fixed)	[47]
	Chabazite	2.0	$K_o = 62 \pm 1$	4 (fixed)	[48]
Zeolitic Material with 6-membered rings	Nepheline	1.0	$K_o = 47.32 \pm 0.26$	2.77 ± 0.24	[49]
Non-ABC-6 family zeolites	Na—P1	1.0	$K_o = 63.8 \pm 0.2$	4 (fixed)	[50]
	Analcime	2.0	$K_o = 56 \pm 3$	4 (fixed)	[51]
	Faujasite	2.4	$K_o = 36.3 \pm 1.2$	4 (fixed)	[52]
	A (=4A)	1.0	$K_o = 22.1 \pm 0.3$	4 (fixed)	[53]
Unreacted fly ash phases	Quartz (α)	–	$K_o = 37.1 \pm 0.2$	6 ± 1	[54]
	Mullite	–	$K_o = 169.1–173.6$	–	[55]
	Fly ash (solid)	–	$E = 98$ (for 5–10 μm size) – 126 (for 150–250 μm size)	–	[56]
	Fly ash (hollow)	–	$E = 13–17$ (for all particle sizes)	–	

Note: sodalite and nepheline comprises only 6-rings as same as hydroxycancrinite; whereas chabazite (or herschelite) is made up of double 6-rings; the value for analcime was measured below 1 GPa; faujasite was measured below 2 GPa; * = current study.

References

[1] Palomo A, Grutzeck MW, Blanco MT. Alkali-activated fly ashes: a cement for the future. Cem Concr Res 1999;29:1323–9.
[2] Davidovits J. Synthesis of new high-temperature geo-polymers for reinforced plastics, composites. SPE PACTEC. 1979;79:151–4.
[3] Palomo A, Alonso S, Fernandez-Jiménez A, Sobrados I, Sanz J. Alkaline activation of fly ashes: NMR study of the reaction products. J Am Ceram Soc 2004;87:1141–5.
[4] Krivenko PV, Kovalchuk G Yu. Heat-resistant fly ash based geocements. In: Proceedings of the international conference on geopolymer 28th–29th October 2002, Melbourne, Australia; 2002.
[5] Criado M, Palomo A, Fernández-Jiménez A. Alkali activation of fly ashes. Part 1: Effect of curing conditions on the carbonation of the reaction products. Fuel 2005;84:2048–54.
[6] Bakharev T. Durability of geopolymer materials in sodium and magnesium sulfate solutions. Cem Concr Res 2005;35:1233–46.
[7] Bakharev T. Geopolymeric materials prepared using class F fly ash and elevated temperature curing. Cem Concr Res 2005;35:1224–32.
[8] Fernandez-Jimenez A, Palomo A, Criado M. Microstructure development of alkali-activated fly ash cement: a descriptive model. Cem Concr Res 2005;35:1204–9.
[9] Bakharev T. Thermal behaviour of geopolymers prepared using class F fly ash and elevated temperature curing. Cem Concr Res 2006;36:1134–47.
[10] Criado M, Fernández-Jiménez A, de la Torre AG, Aranda MAG, Palomo A. An XRD study of the effect of the SiO2/Na2O ratio on the alkali activation of fly ash. Cem Concr Res 2007;37:671–9.
[11] Dombrowski K, Buchwald A, Weil M. The influence of calcium content on the structure and thermal performance of fly ash based geopolymers. J Mater Sci 2007;42:3033–43.
[12] Fernández-Jiménez A, García-Lodeiro I, Palomo A. Durability of alkali-activated fly ash cementitious materials. J Mater Sci 2007;42:3055–65.
[13] Alvarez-Ayuso E, Querol X, Plana F, Alastuey A, Moreno N, Izquierdo M, et al. physical and structural characterisation of geopolymer matrixes synthesised from coal (co-) combustion fly ashes. J Hazard Mater 2008;154:175–83.
[14] Oh J, Monteiro PJM, Jun SS, Choi S, Clark SM. The evolution of strength and crystalline phases for alkali-activated ground blast furnace slag and fly ash-based geopolymers. Cem Concr Res 2010;40:189–96.
[15] Cejka J, Van Bekkum H, Corma A, Schuth F, editors. Introduction to zeolite science and practice. Amsterdam: Elsevier; 2007.
[16] Fernández-Jiménez A, Palomo A, Sobrados I, Sanz J. The role played by the reactive alumina content in the alkaline activation of fly ashes. Micropor Mesopor Mater 2006;91:111–9.
[17] Khale D, Chaudhary R. Mechanism of geopolymerization and factors influencing its development: a review. J Mater Sci 2007;42:729–46.
[18] Querol X, Moreno N, Umana J, Alastuey A, Hernández E, Lopez-Soler A, et al. Synthesis of zeolites from coal fly ash: an overview. Int J Coal Geology 2002;50:413–23.
[19] Wałek TT, Saito F, Zhang Q. The effect of low solid/liquid ratio on hydrothermal synthesis of zeolites from fly ash. Fuel 2008;87:3194–9.
[20] Inada M, Eguchi Y, Enomoto N, Hojo J. Synthesis of zeolite from coal fly ashes with different silica–alumina composition. Fuel 2005;84:299–304.
[21] Querol X, Alastuey A, Lopez-Soler A, Plana F, Andres JM, Juan R, et al. A fast method for recycling fly ash: microwave-assisted zeolite synthesis. Environ Sci Technol 1997;31:2527–33.
[22] Zeng R, Umana J, Querol X, Lopez-Soler A, Plana F, Zhuang X. Zeolite synthesis from a high Si—Al fly ash from East China. J Cheml Technol Biotechnol 2002;77:267–73.
[23] Pacheco-Torgal F, Castro-Gomes J, Jalali S. Alkali-activated binders: a review. Part 2. About materials and binders manufacture. Constr Build Mater 2008;22:1315–22.
[24] Bonaccorsi E, Merlino S. Modular microporous minerals: cancrinite-davyne group and CSH phases. Rev Mineral Geochem 2005;57:241–90.
[25] Khomyakov AP, Nadezhina TN, Rastsvetaeva RK, Pobedimskaya EA. Hydroxycancrinite Na_8 $[Al_6Si_6O_{24}](OH)_2$—$2H_2O$:A new mineral. Zap Veseross Mineral Obs 1992;121:100–5.
[26] Němeček J, Šmilauer V, Kopecký L. Characterization of alkali-activated fly-ash by nanoindentation. Nanotechnol Construct 2009;3:337–43.
[27] Škvára F, Kopecký L, Nemecek J, Bittnar Z. Microstructure of geopolymer materials based on fly ash. Ceramics–Silikáty 2006;50:208–15.
[28] Duxson P, Mallicoat SW, Lukey GC, Kriven WM, Van Deventer JSJ. The effect of alkali and Si/Al ratio on the development of mechanical properties of metakaolin-based geopolymers. Colloids Surf Physicochem Eng Aspects 2007;292:8–20.
[29] Pacheco-Torgal F, Castro-Gomes J, Jalali S. Properties of tungsten mine waste geopolymeric binder. Constr Build Mater 2008;22:1201–11.
[30] Kirschner AV, Harmuth H. Investigation of geopolymer binders with respect to their application for building materials. Ceramics–Silikáty 2004;48:117–20.
[31] Sofi M, Van Deventer JSJ, Mendis PA, Lukey GC. Engineering properties of inorganic polymer concretes (IPCs). Cem Concr Res 2007;37:251–7.
[32] Duxson P, Provis JL, Lukey GC, Mallicoat SW, Kriven WM, van Deventer JSJ, et al. Understanding the relationship between geopolymer composition, microstructure and mechanical properties. Colloids Surf Physicochem Eng Aspects 2005;269:47–58.
[33] Bell J, Gordon M, Kriven W. Nano-and microporosity in geopolymer gels. Microsc Microanal 2006;12:552–3.
[34] Trtik P, Münch B, Lura P. A critical examination of statistical nanoindentation on model materials and hardened cement pastes based on virtual experiments. Cem Concr Compos 2009;31:705–14.
[35] Kunz M, MacDowell AA, Caldwell WA, Cambie D, Celestre RS, Domning EE, et al. A beamline for high-pressure studies at the Advanced Light Source with a superconducting bending magnet as the source. J Synchrotron Radiat 2005;12:650–8.
[36] Hammersley AP. Fit2d version 12.040, ESRF, Grenoble, France; 2006.
[37] Cheary RW, Coelho AA. Programs XFIT and FOURYA, deposited in CCP14 powder diffraction library. Warrington, England: Engineering and Physical Sciences Research Council, Daresbury Laboratory; 1996. <http://www.ccp14.ac.uk/tutorial/xfit-95/xfit.htm>.
[38] Angel RJ, Bujak M, Zhao J, Gatta GD, Jacobsen SD. Effective hydrostatic limits of pressure media for high-pressure crystallographic studies. J Appl Cryst 2007;40:26–32.
[39] Mao HK, Xu J, Bell PM. Calibration of the ruby pressure gauge to 800 kbar under quasi-hydrostatic conditions. J Geophys Res 1986;91:4673–6.
[40] Laugier J, Bochu B. CELREF. Version 3. Cell parameter refinement program from powder diffraction diagram. France: Laboratoire des Matériaux et du Génie Physique, Ecole Nationale Supérieure de Physique de Grenoble (INPG); 2002.
[41] Birch F. Finite strain isotherm and velocities for single-crystal and polycrystalline NaCl at high pressures and 300 K. J Geophys Res 1978;83:1257–68.
[42] Meade C, Jeanloz R. Static compression of Ca (OH) 2 at room temperature-observations of amorphization and equation of state measurements to 10.7 GPa. Geophys.Res.Lett. 1990;17:1157–60.
[43] Jeanloz R. Finite-strain equation of state for high-pressure phases. Geophys Res Lett 1981;8:1219–22.
[44] Knittle E. Static compression measurements of equations of state. Miner Phys Crystallogr: A Handbook Phys Constants 1995:98–142.
[45] Gatta GD. Does porous mean soft? On the elastic behaviour and structural evolution of zeolites under pressure. Z Kristallogr 2008;223:160–70.
[46] Reed BC. Linear least-squares fits with errors in both coordinates. II: Comments on parameter variances. Am J Phys 1992;60:59–62.
[47] Hazen RM, Sharp ZD. Compressibility of sodalite and scapolite. Am Mineral 1988;73:1120–2.
[48] Leardini L, Quartieri S, Vezzalini G. Compressibility of microporous materials with CHA topology: 1. Natural chabazite and SAPO-34. Micropor Mesopor Mater 2010;127:219–27.
[49] Gatta GD, Angel RJ. Elastic behavior and pressure-induced structural evolution of nepheline: Implications for the nature of the modulated superstructure. Am Mineral 2007;92:1446–55.
[50] Betti C, Fois E, Mazzucato E, Medici C, Quartieri S, Tabacchi G, et al. Gismondine under HP: deformation mechanism and re-organization of the extra-framework species. Micropor Mesopor Mater 2007;103:190–209.
[51] Gatta GD, Nestola F, Ballaran TB. Elastic behavior, phase transition, and pressure induced structural evolution of analcime. Am Mineral 2006;91:568–78.
[52] Isambert A, Angot E, Hébert P, Haines J, Levelut C, Parc RL, et al. Amorphization of faujasite at high pressure: an X-ray diffraction and Raman spectroscopy study. J Mater Chem 2008;18:5746–52.
[53] Arletti R, Ferro O, Quartieri S, Sani A, Tabacchi G, Vezzalini G. Structural deformation mechanisms of zeolites under pressure. Am Mineral 2003;88:1416–22.
[54] Jorgensen JD. Compression mechanisms in α-quartz structures—SiO2 and GeO_2. J Appl Phys 1978;49:5473–8.
[55] Schneider H, Schreuer J, Hildmann B. Structure and properties of mullite – a review. J Euro Ceram Soc 2008;28:329–44.
[56] Matsunaga T, Kim JK, Hardcastle S, Rohatgi PK. Crystallinity and selected properties of fly ash particles. Mater Sci Eng A 2002;325:333–43.